Thermal Science and Engineering Progress 50 (2024) 102542

Contents lists available at ScienceDirect

Thermal Science and Engineering Progress

journal homepage: www.sciencedirect.com/journal/thermal-science-and-engineering-progress

Performance simulation of metal hydride based flat coupled beds with differential sizes for cooling/heating

Biju John Koshy [a], G. Mohan [a,*], M. Prakash Maiya [b]

[a] Center for Computational Research in Clean Energy Technologies, Sree Chitra Thirunal College of Engineering (Affiliated to APJ Abdul Kalam Technological University), Thiruvananthapuram 695018, India
[b] Refrigeration and Air Conditioning Lab, Indian Institute of Technology Madras, Chennai 600036, India

ARTICLE INFO

Keywords:
Metal Hydride
Cooling System
Simulation

ABSTRACT

Hydrogen being the most abundant element in the universe has great potential towards decarbonisation at the point of usage. Metal hydride-based heat pumps/ refrigerators are getting increasing acceptance due to its environment friendliness and safety. These systems operate over a wide range of temperatures and pressures. The thermal performance of these systems depends mainly on the reaction kinetics of the alloy pairs. Difference in the reaction rates of the alloy pairs, causes a certain amount of hydride to go unutilized during cycling. While a variety of reactor designs and heat transfer enhancements are suggested, optimal thermal design of coupled beds with minimum weight and cycle time remains a major challenge. In the present study, numerical simulation of differently sized coupled beds based on the alloy pair of $LaNi_{4.7}Al_{0.3}$ - $La_{0.8}Ce_{0.2}Ni_5$ is carried out using COMSOL Multiphysics® commercial code. The effect of mass ratio on the hydrogen pressure and hydride concentration in the coupled bed is highly significant. It is found that 12 % increase in COP (0.28) is obtained for a cycle time of 260 s and mass ratio of 1.5. This corresponds to minimum alloy weight ensuring effective transfer of hydrogen across HT-LT reactors.

1. Introduction

Hydrogen has great potential towards decarbonisation [1]. Metal hydride based heating and cooling systems are thermally driven and operate similar to conventional sorption systems [2,3]. Formation of metal hydride is an exothermic reaction while supply of heat can lead to the breaking of bonds to liberate hydrogen. The unique advantage of these systems is that any operational temperature can be realised by suitably changing the alloy composition [4,5].

Nishizaki et al. [6] introduced the concept of sensible heating/ cooling in the working cycle in a model developed to analyse the performance of a metal hydride heat pump. Maximum performance is associated with flat plateau, low reactor heat capacities and efficient heat interaction [6]. In a review of metal hydride based heating and cooling systems [3], the operating principles of the various systems and suggestions for the improvement of the coefficient of performance and specific cooling capacity were presented. An extensive study [7] on the materials used in hydride chemical heat pumps for cooling and heating applications were reported.

Tyler et al. [8] observed that hydride pairs having high hydriding enthalpies could achieve reasonable performance even with relatively low hydrogen transfer between them. Experimental analysis on the reaction kinetics of various AB_5 alloys of different bed thickness [9] proposed aluminium foam as a heat transfer enhancement method and stressed the influence of extremely porous aluminium foam on the reaction kinetics. Addition of catalyst into the metal hydrides, alloying the metal hydrides and nano-structuring improved the absorption/ desorption properties of hydrogen [10]. Material characterisation of $La_{0.9}Ce_{0.1}Ni_5$, $La_{0.8}Ce_{0.2}Ni_5$, $LaNi_{4.7}Al_{0.3}$ and $LaNi_{4.6}Al_{0.4}$ to determine their suitability in metal hydride based cooling systems, conducted by Sharma and Kumar [11] revealed that higher the pressure difference between the metal hydride beds, higher would be the cooling capacity in shorter cycle times. A study [12] on the properties of $LaNi_{5-x}Al_x$ ($x = 0.3$, 0.4) calculated the enthalpy of formation and entropy of formation using vant' Hoff equation [13] and the effects of Al content on the properties were analysed. The reaction kinetics of certain La based metal hydrides were analysed to determine their suitability for cooling systems [14].

Many studies based on metal hydride beds having a cylindrical geometry have been reported [15–21]. Satheesh et al. [15] used fully implicit finite volume method to predict the heat and mass transfer characteristics between the coupled beds, using alloy pair of

* Corresponding author.
E-mail address: mohan.g.menon@sctce.ac.in (G. Mohan).

https://doi.org/10.1016/j.tsep.2024.102542
Received 29 November 2023; Received in revised form 14 February 2024; Accepted 18 March 2024
Available online 21 March 2024

Nomenclature

T	temperature, K
P	pressure, Pa
c	concentration of hydride, mol m^{-3}
C_p	specific heat, J kg^{-1} K^{-1}
E	activation energy, J mol^{-1}
R	universal gas constant, 8.314 J mol^{-1} K^{-1}
k	thermal conductivity, W m^{-1} K^{-1}
C	material dependant constant, s^{-1}
d	diameter, m
COP	co-efficient of performance

Greek Letters

ΔH^0	heat of formation, J kg^{-1}
μ	dynamic viscosity, kg m^{-1} s^{-1}
ε	porosity
ρ	density, kg m^{-3}
K	permeability, m^2

Subscripts

a	absorption
d	desorption
e	effective
eq	equilibrium
sat	saturation
s	solid
A	reactor A
B	reactor B
p	particle
MR	Mass ratio

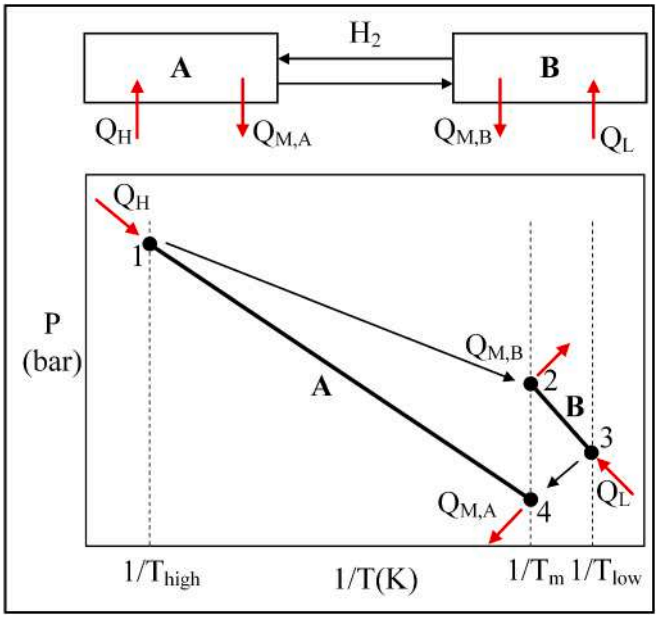

Fig. 1. van't Hoff plot for single stage metal hydride based coupled beds.

$MmNi_{4.6}Al_{0.4}$ /$MmNi_{4.6}Fe_{0.4}$. They used transient, 2D mathematical model in an annular cylindrical configuration for analysis and reported variation in hydrogen concentration, temperature distribution and equilibrium pressure. The difference in cycle times for variable and constant wall temperature boundary conditions were approximately 5mins. The lowest refrigeration temperature observed was 269.1 K. The numerical study [16], evaluated the performance of a single stage metal hydride-based heat transformer in which the alloy pair of $LaNi_5$ and $LaNi_{4.7}Al_{0.3}$ was considered for the analysis. The effect of operating temperatures namely, heat source, and heat output and heat rejection temperatures on the performance of the system were reported. The performance enhanced with increase in heat source temperature while it decreased with increase in heat output temperature. For a given thermal conductivity, the cycle time was reduced by 30 % by reducing the bed thickness [16]. In the performance analysis of a single stage metal hydride heat pump working with five different alloy pairs, the maximum COP obtained was 0.66 and the highest specific cooling power of total hydride mass obtained was 53.25 W/kg [17]. The simulation study [18] of double stage metal hydride heat pump showed the variation in hydrogen concentrations, hydride equilibrium pressures and heat transferred for one complete cycle. For the given operating conditions, the study reported a COP of 0.471 and specific cooling power (SCP) of 28.4 W/kg of total hydride mass. Malleswararao et al. [19] conducted 3D simulation of coupled Mg_2Ni-$LaNi_5$ using COMSOL Multiphysics®, using an alloy pair of Mg_2Ni and $LaNi_5$ and discussed the thermodynamic compatibility criteria for the selection of metal hydride pairs. The same team conducted studies [20] on long term and buffer modes of operations of a thermal energy storage system using the same alloy pair. Two interconnected cylindrical reactors were simulated using COMSOL Multiphysics®, to find the effect of heat source temperature on the thermal performance of system. The feasibility and performance analysis of a thermal energy storage system was conducted [21] based on the alloy pair of $NaMgH_2F$ and $TiCr_{1.6}Mn_{0.2}$ integrated with a solar driven ultra-supercritical steam power plant. The transport of hydrogen was modelled using COMSOL Multiphysics®. High temperature operating condition was of the order of 600 °C. The results indicated the potential of the system to provide high energy densities with heat transfer limitations being the critical parameter for system design.

A review by Murthy [22] on the heat and mass transfer in solid-state hydrogen storage discussed the effect of pressure, concentration, number of cycles and particle decay on the effective thermal conductivity of the bed. Another detailed review [23] on the modelling methods for heat transfer during charging and discharging of MH tank in a coupled system, active and passive thermal management, and thermal coupling methods, emphasize the adoption of right thermal management techniques to improve the gravimetric storage and flow of hydrogen between the reactor beds. Experimental characterisation [24] using metal hydride hydraalloy reported cycle time under one minute. Results showed that the plate reactor concept is feasible for all metal hydride applications if the parasitic reactor mass is reduced and external heat transfer is increased. Numerical study, comparing the results with the experimental work, helped to find out optimum thickness of the reactor for the application considering an open cooling system [25]. Studies on a metal hydride based year round comfort heating and cooling system for extreme climates [26] showed the effects of system parameters on the performance of the system using the alloy pair of $Zr_{0.82}Mm_{0.09}Ti_{0.09}Fe_{1.4}Cr_{0.6}$ – $LaNi_{4.6}Al_{0.4}$. Storage capacity of absorption/desorption of hydrogen of the two metal hydrides considered were different. Alloy having lower sorption kinetics was considered **as** the rate controlling factor. Differential masses of reactors were used to improve the performance. Maximum COP was obtained for a mass ratio of 1.83. Difference in the reaction rates of the alloy pairs can cause a certain amount of hydride remain unutilized during cycling or may lead to a pressure build up. The build-up of hydrogen pressure should also be minimum. One way to achieve it is by using differential masses of two hydrides.

Development of thermal design of coupled beds for heating/ cooling

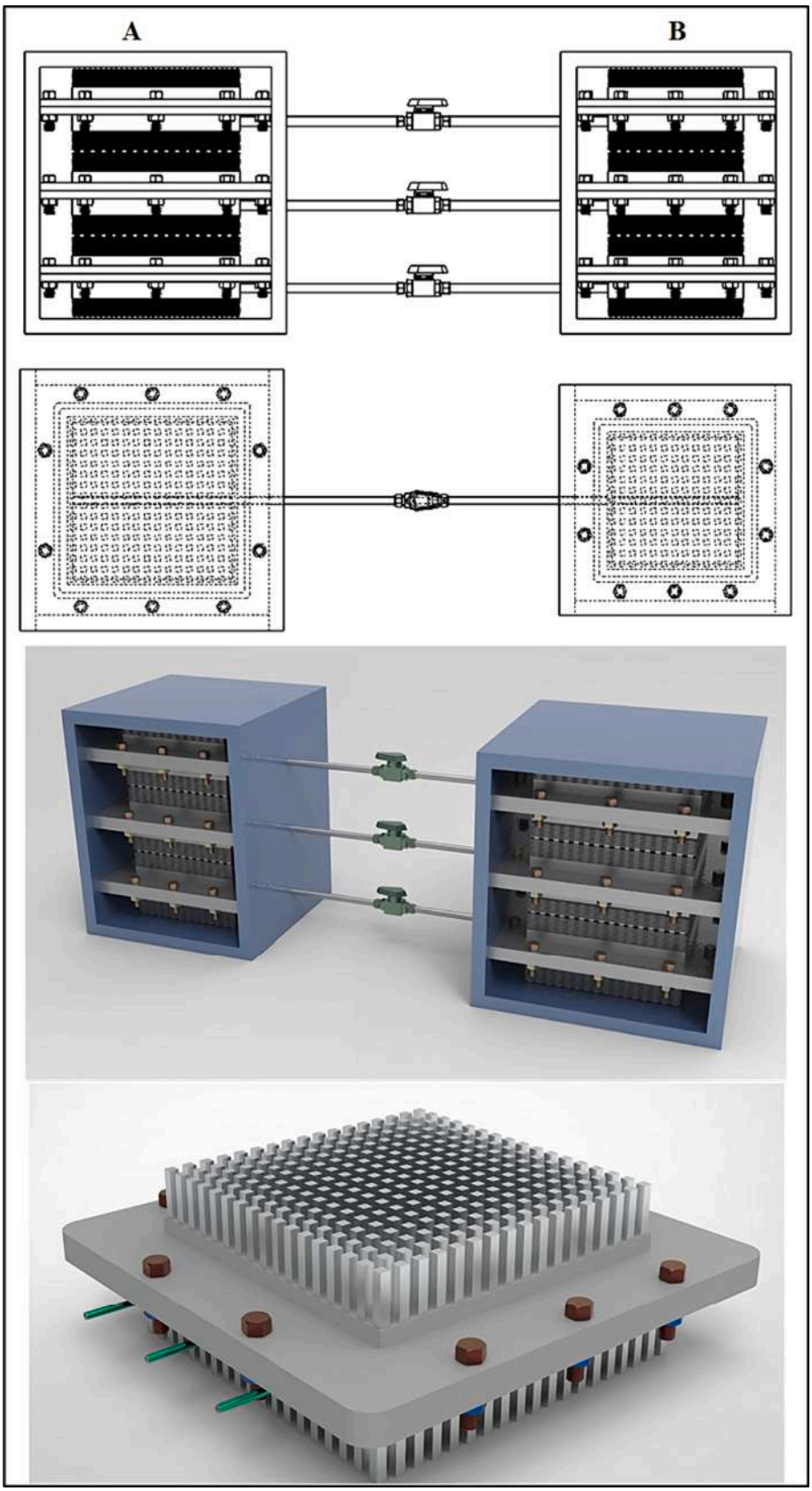

Fig. 2. Schematic of stacking arrangement of metal hydride based flat plate coupled reactors. HT reactor A filled with $LaNi_{4.7}Al_{0.3}$ and LT Reactor B filled with $La_{0.8}Ce_{0.2}Ni_5$.

application depends on the reactor geometry, heat transfer surface area and thermal management systems [22–26]. These factors need to be optimized within the constraints of application, which include total system weight and targeted cycle time. Though several studies have been done on the thermal performance of these systems, the effect of differential masses of alloy pairs having similar absorption /desorption capacity on the system performance have not been reported. In this study, we conducted numerical simulation of hydrogen transport between differently sized coupled beds based on the alloy pair of $LaNi_{4.7}Al_{0.3}$ - $La_{0.8}Ce_{0.2}Ni_5$.

2. Methodology

The operating principle of a metal hydride based coupled beds is shown on the vant' Hoff plot (Fig. 1). The refrigeration cycle consists of two heat and mass transfer processes (1–4 and 2–3) and two sensible heating/cooling processes (1–2 and 3–4). The cycle works between three temperature limits, high temperature (T_{high}), intermediate temperature (T_m) and low temperature (T_{low}). Initially reactor A is considered to be fully hydrided and kept at temperature T_{high}. Reactor B is fully dehydrided and kept at T_m. At this state there exist an equilibrium pressure difference between the two reactors. Equilibrium pressure of a reactor is a function of its temperature. Once the valve is opened, hydrogen gets desorbed from reactor A and travels towards reactor B, where it gets absorbed. While desorbing, the reactor A is supplied heat (Q_H) using the heat transfer fluid to meet the required heat of reaction. While absorbing, the reactor B rejects heat ($Q_{M,B}$) to the bed and heat transfer fluid. This process is called regeneration. The process continues until certain amount of hydrogen is transferred between the reactors. Then, the valves are closed and both the reactors are sensibly cooled. Reactor A is cooled to T_m and reactor B is cooled to T_{low}. Once the valve is opened, hydrogen is desorbed from reactor B and gets absorbed in Reactor A. During desorption, the heat of reaction is taken from the bed and heat transfer fluid. This gives the refrigerating effect (Q_L). This process is called refrigeration. During this process reactor A rejects heat ($Q_{M,A}$) while absorbing hydrogen. Then both the reactors are sensibly heated to initial temperatures.

2.1. Physical model

Fig. 2, represents the schematic of a pair of metal hydride based flat plate reactors. The physical model consists of two flat plate reactors A and B of square cross section. The reactors are filled with the metal hydrides. Reactor A is filled with the high temperature alloy (HT alloy) and reactor B is filled with the low temperature alloy (LT alloy). They are connected together by means of a connecting pipe, which has a control valve to regulate the flow of hydrogen between them. The coupled reactors are stacked on top of each other using square pin fins. Stacking provides structural integrity and improved packing density. Stacked reactors are enclosed in a duct through which the heat transfer fluid flows. Air is considered as the heat transfer fluid. Air at the required temperature is passed over the flat plate reactors through ducts with an entry velocity of 3 m/s.

The following assumptions were made to simplify the problem:

1. Effect of plateau slope and hysteresis have on sorption kinetics are neglected.
2. Thermo-physical properties are independent of the pressure, bed temperature and concentration.
3. Conduction is the prevalent mode of heat transfer within the bed.
4. Natural convection and radiation effects within the bed are neglected.
5. Hydride bed has uniform porosity.
6. Mechanical effects due to pulverization, swelling/shrinkage, settling and agglomeration during cycling are negligible.

2.2. Problem formulation

2.2.1. Mass balance of metal

Hydrogen entering the rector bed gets converted to metal hydride with associated changes in density.

Conservation of mass for the solid phase of reactor is expressed as

$$(1-\varepsilon)\frac{\partial \rho_s}{\partial t} = \dot{m} \tag{1}$$

$\dot{m}$ is the rate of gas absorbed

2.2.2. Sorption kinetics

The amount of hydrogen absorbed is expressed as

$$\dot{m} = -C_a exp(-\frac{E_a}{RT}) ln(\frac{P}{P_{eq}})(\rho_{sat}-\rho_s) \tag{2}$$

The amount of hydrogen desorbed per unit time and unit volume is expressed as

$$\dot{m} = -C_d \exp(-\frac{E_d}{RT})(\frac{P-P_{eq}}{P_{eq}})\rho_s \tag{3}$$

Equilibrium pressure is determined by van't Hoff relationship

$$\ln(P_{eq}) = A - \frac{B}{T} \tag{4}$$

A and B are van't Hoff constants

2.2.3. Energy balance

Heat generated due to exothermic reaction causes associated spatial temperature imbalances within the bed. Energy conservation equation in the hydride is given by

$$(\rho C_P)_e \frac{\partial T}{\partial t} = k_e \frac{\partial}{\partial x}(\frac{\partial T}{\partial x}) + k_e \frac{\partial}{\partial y}(\frac{\partial T}{\partial y}) + k_e \frac{\partial}{\partial z}(\frac{\partial T}{\partial z}) - \dot{m}\Delta H^0 \tag{5}$$

The right hand term represents the heat of reaction and spatial variation of temperature.

2.2.4. Momentum balance

Momentum balance for the flow of hydrogen can be expressed by the Brinkman equation (Eq. (6))

$$\begin{aligned}
\frac{\partial}{\partial x}\left(\mu\frac{\partial u}{\partial x}\right) + \frac{\partial}{\partial y}\left(\mu\frac{\partial u}{\partial y}\right) + \frac{\partial}{\partial z}\left(\mu\frac{\partial u}{\partial z}\right) - \mu K u_x &= -\frac{\partial p}{\partial x} + F_X \\
\frac{\partial}{\partial x}\left(\mu\frac{\partial v}{\partial x}\right) + \frac{\partial}{\partial y}\left(\mu\frac{\partial v}{\partial y}\right) + \frac{\partial}{\partial z}\left(\mu\frac{\partial v}{\partial z}\right) - \mu K u_y &= -\frac{\partial p}{\partial y} + F_y \\
\frac{\partial}{\partial x}\left(\mu\frac{\partial w}{\partial x}\right) + \frac{\partial}{\partial y}\left(\mu\frac{\partial w}{\partial y}\right) + \frac{\partial}{\partial z}\left(\mu\frac{\partial w}{\partial z}\right) - \mu K u_z &= -\frac{\partial p}{\partial z} + F_z
\end{aligned} \tag{6}$$

F_X, F_y, F_z– Body forces per unit volume

Permeability (K) is calculated using the Kozeny-Carman equation

$$\mathrm{K} = \frac{{d_p}^2 \varepsilon^3}{150^*(1-\varepsilon)^2} \tag{7}$$

The performance of a metal hydride based coupled bed are characterized by the COP. It is defined as:

$$COP = \frac{Q_L}{Q_H} \tag{8}$$

Q_L is the refrigeration effect and Q_H is the heat input.

2.3. Simulation methodology

The transfer of hydrogen between the reactors, as well as the heat

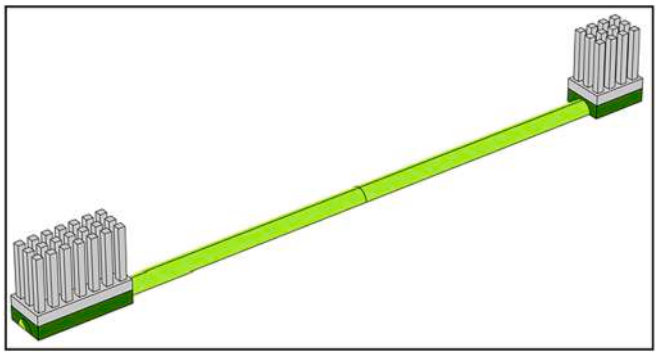

Fig. 3. Simulation model of metal hydride based flat plate coupled reactors.

Table 1
Geometric parameters values used in present simulation study.

Geometric parameter	Values
Fin thickness (mm)	2
Inter-spacing between two fins (mm)	2
Height of fin (mm)	15
Length of connecting tube (mm)	150
Diameter of connecting pipe (mm)	6
Bed thickness (mm)	4

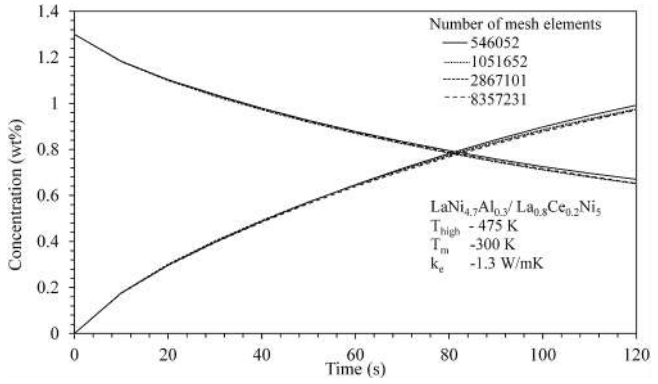

Fig. 4. Grid Independence study for metal hydride based flat plate coupled reactors.

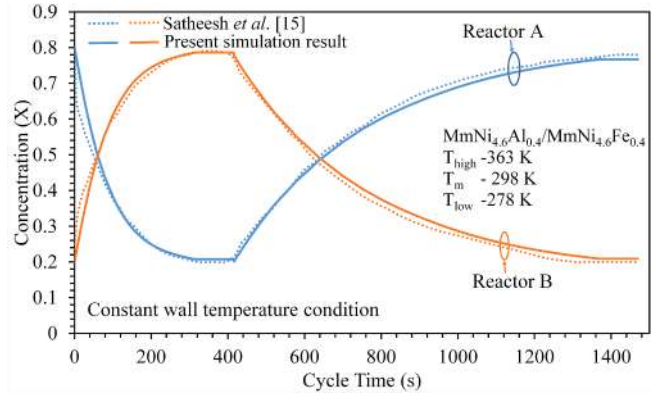

Fig. 5. Validation of present simulation model with results of Satheesh et al. [15].

interactions between the reactor beds and the heat transfer fluid, are predicted by solving the conservation equations for mass, momentum, and energy. In- built modules in COMSOL Multiphysics®, namely

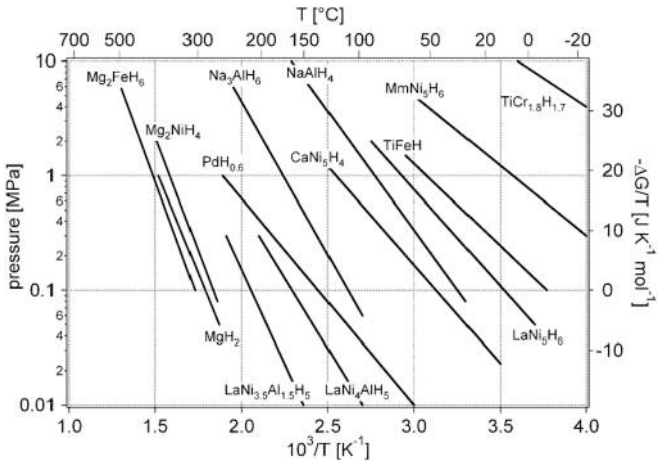

Fig. 6. van't Hoff plot of some selected hydrides [27].

Table 2
Operating conditions considered in present simulation study.

Operating conditions	Values
High temperature (K)	475
Intermediate temperature (K)	300
Low temperature (K)	283
Velocity of air at inlet of air domain (m/s)	3

Table 3
Thermo-physical properties of alloy pair [3,28].

Thermo-physical properties of alloy pair		$La_{0.8}Ce_{0.2}Ni_5$	$LaNi_{4.7}Al_{0.3}$
Specific heat (J/kg K)		419	419
Thermal conductivity (W/m K)		1.3	1.3
Activation energy	Ea (J/mol)	21179.6	29,210
	Ed (J/mol)	16,420	28,490
Density (kg/m^3)		8200	8200
Porosity		0.5	0.5
Particle diameter (μm)		20	20
Permeability (m^2)		10^{-12}	10^{-12}
Enthalpy of reaction (J/mol)		23,800	34,000
Entropy of reaction (J/mol K)		108	106.8
Reaction constants	Cd (1/s)	9.57	8.2
	Ca (1/s)	59.187	43.27

Transport of diluted species in porous media, Heat transport in porous media were used to implement the conservation of mass and energy of hydride beds. Airflow was simulated considering laminar flow. The size of the LT alloy was kept constant. The size of HT alloy was varied to vary the mass ratio of HT alloy to LT alloy from 1 to 2.5. The length along the direction of air flow was kept constant in all cases for both reactors. Fig. 3 represents the simulation model of metal hydride based flat plate coupled reactors. Table 1, shows the geometric parameters used in simulation study. The bed thickness of 4 mm was kept constant. A grid independence test was conducted by varying the element size. Fig. 4 shows the variation in concentration for different grid sizes. Based on this, optimised grid size is determined. Physics-controlled mesh feature was used initially to generate the mesh elements, but to enhance the mesh quality, the element size was subsequently reduced. The model was solved using a segregated solver. The simulation was run for two cycles. The cycle time of 260 s is considered. It includes four processes denoted as a, b, c, and d: regeneration (120 s), sensible cooling (40 s), refrigeration (60 s), and sensible heating (40 s).

2.4. Validation of the numerical model

For validation purpose, reactor geometry and operating conditions

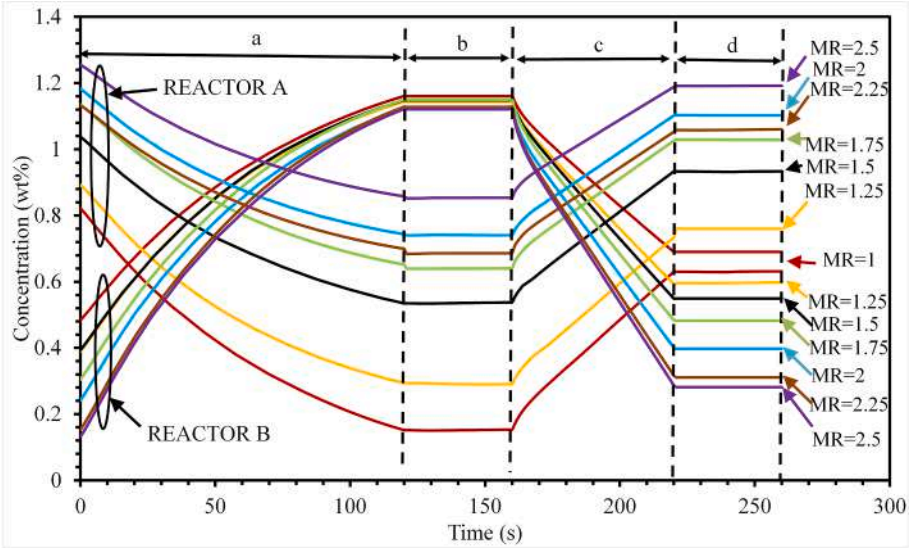

Fig. 7. Effect of mass ratio (M_{HT}/M_{LT}) on hydrogen concentration. T_{high} = 475 K, T_m = 300 K and T_{low} = 283 K (a- Regeneration, b- Sensible Cooling, c- Refrigeration, d- Sensible heating).

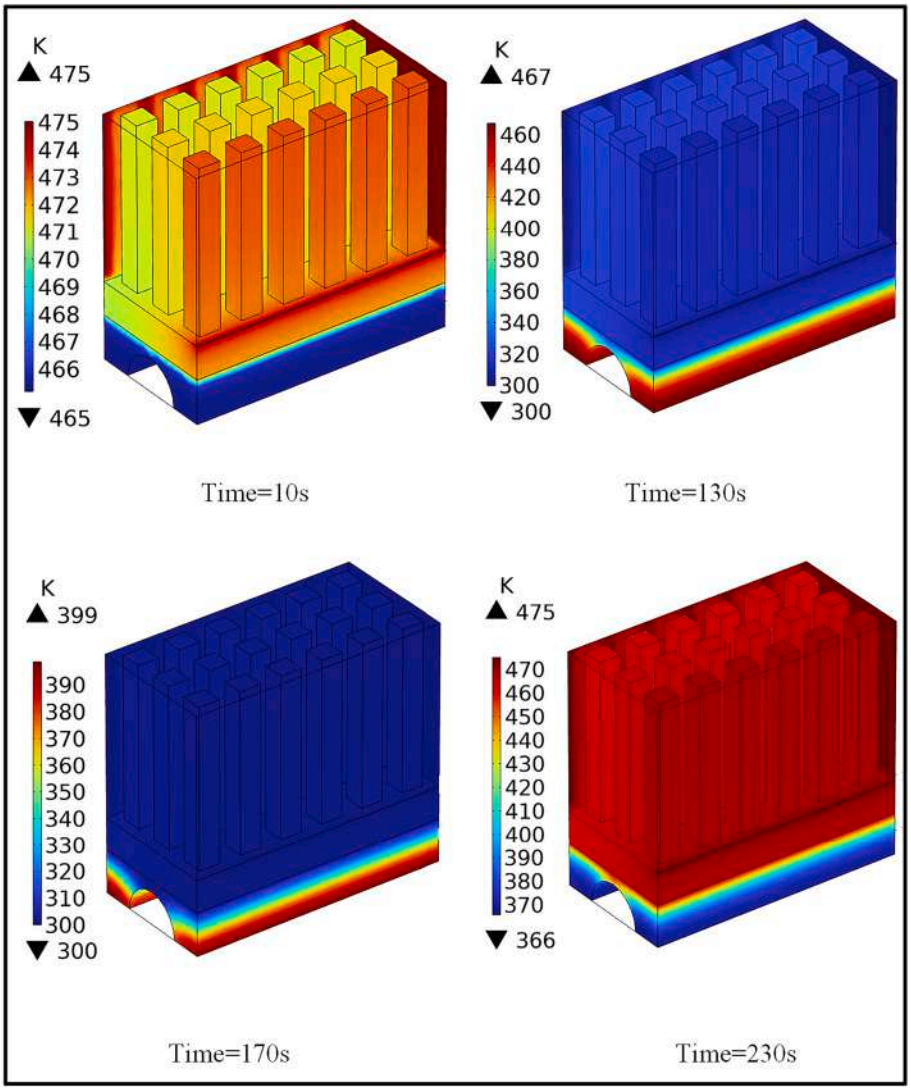

Fig. 8a. Spatial variation of surface temperature of HT side at different time intervals. MR = 1.5. T_{high} = 475 K, T_m = 300 K and T_{low} = 283 K.

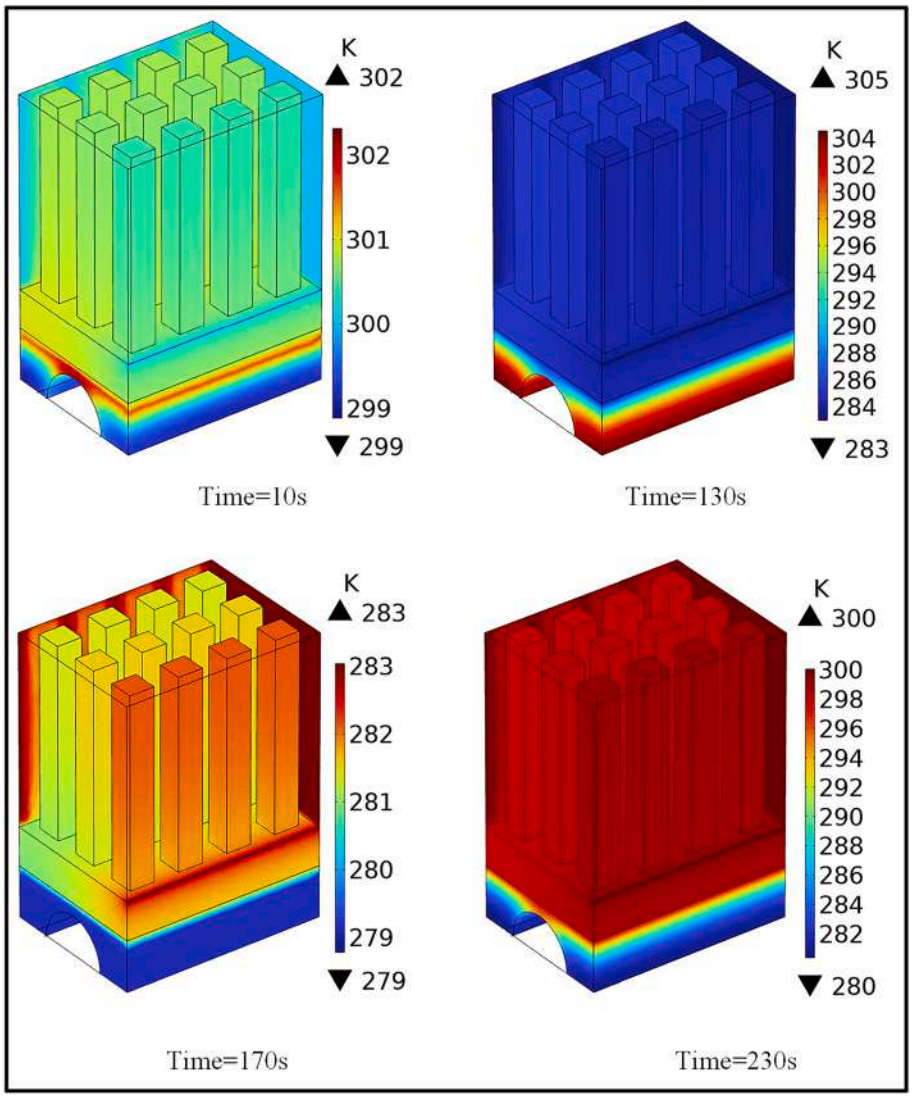

Fig. 8b. Spatial variation of surface temperature of LT side at different time intervals. MR = 1.5. T_{high} = 475 K, T_m = 300 K and T_{low} = 283 K.

used by Satheesh *et al.* [15] is taken and simulation is done accordingly. The cycle time, bed thickness and thermo-physical properties are selected based on the conditions reported [15]. Fig. 5, shows the variation of hydrogen concentration in both the reactors with time. The result obtained match reasonably well with the results reported in the literature for the alloy pair of $MmNi_{4.6}Al_{0.4}$ and $MmNi_{4.6}Fe_{0.4}$. A small deviation between the results is due to the assumed values of reaction constants.

2.5. Material selection for sorption cooling

The alloy pair is selected based on satisfying the following conditions: Functional temperature to be around 30 °C to −10 °C for low temperature (LT) hydride to enable cooling and regeneration temperature to 200 °C for high temperature (HT) hydride. Even if the enthalpy of formation is lower in magnitude, it is important that dissociation takes place in the LT hydride easily. The choice of LT hydride is thus critical in the design of sorption cooling systems. However, lower enthalpy of formation results in more cycles. Fig. 6 shows the ln P vs 1/T relationship for the reaction in the useful pressure range of 0.1 atm to 10 atm. From the van't Hoff plot, we observe that La-Ni-X and Ti Fe X systems satisfy these conditions. Of the two, LaNi-X is well characterised and reaction kinetics is good.

Based on this $LaNi_{(5-x)}Al_x$ (x = 0.2–0.8) is selected as HT hydride and La_{1-x} Ni_5Ce_x (x = 0.05–0.2) as LT hydride as they satisfy the above requirements. The main advantage of La_{1-x} Ni_5 Ce_x and $LaNi_{(5-x)}Al_x$ as LT and HT material respectively is that LT material will absorb and desorb hydrogen at ambient temperature down to −20 °C, while HT material can absorb hydrogen at ambient temperature and desorb at 150–200 °C which can be obtained from the waste heat/solar energy.

3. Results and discussion

The alloy pair of $LaNi_{4.7}Al_{0.3}$ - $La_{0.8}Ce_{0.2}Ni_5$ is considered for analysis. Table 2, represents the operating conditions. The working range of the alloy pair matched the operating conditions. Table 3, represents the thermo-physical properties of alloy pair used for simulation.

3.1. Hydrogenation of coupled beds during regeneration and refrigeration

Fig. 7, represents the variation in hydrogen concentration in reactors A and B. During the regeneration process, the valve is opened, and as a result of the pressure differential, hydrogen is desorbed from the reactor A and absorbed by reactor B. As the mass ratio (M_{HT}/M_{LT}) increases, more amount of hydrogen is desorbed from reactor A and absorbed in reactor B. The process continues for 120 s. During sensible cooling, the

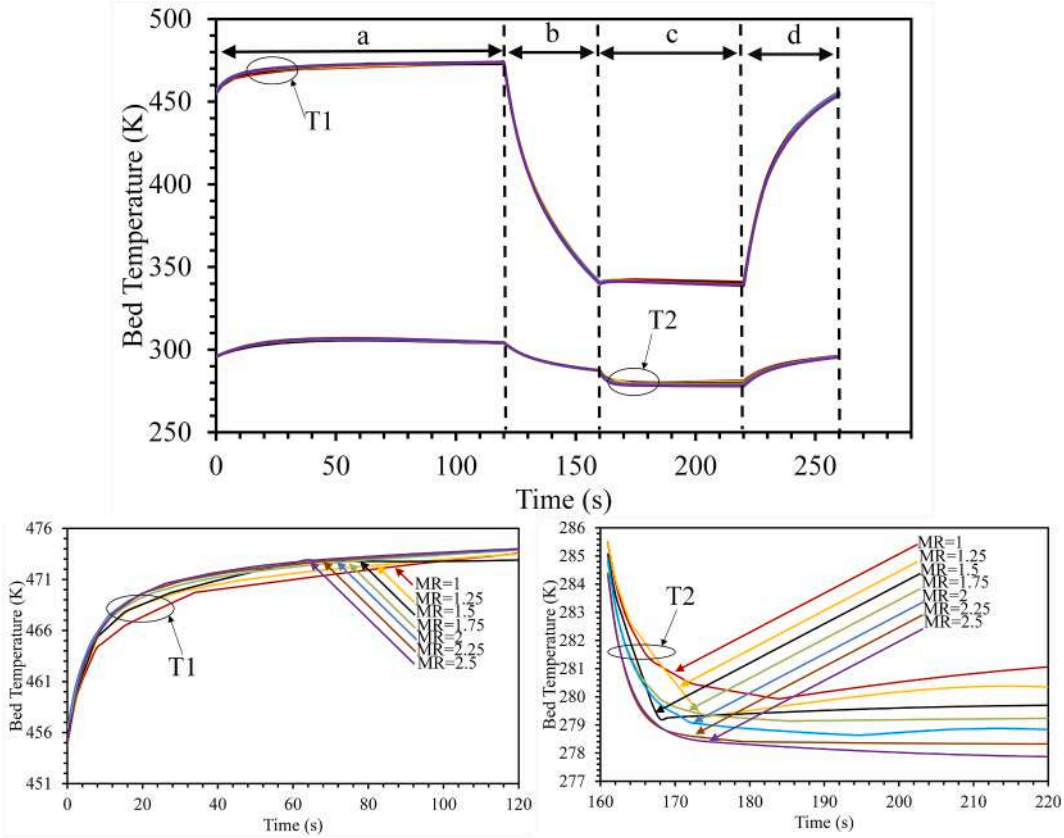

Fig. 9. Effect of mass ratio (MR = M_{HT}/M_{LT}) on the average bed temperature at different time intervals. T_{high} = 475 K, T_m = 300 K and T_{low} = 283 K.

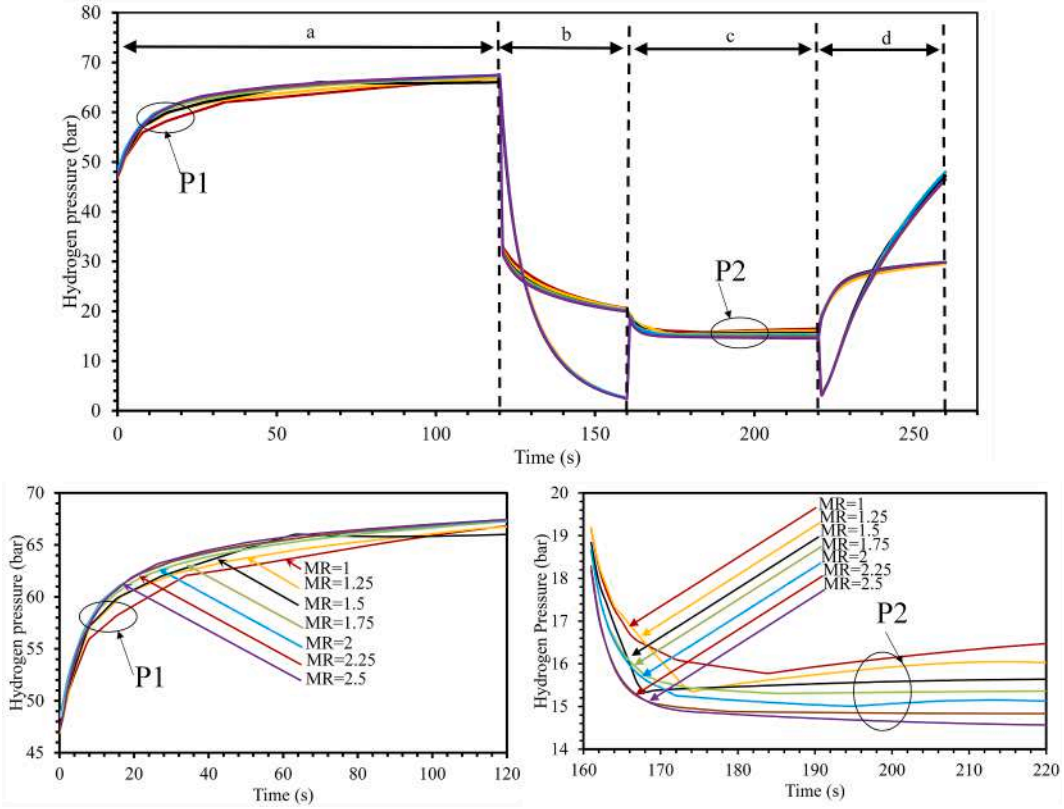

Fig. 10. Effect of mass ratio (MR = M_{HT}/M_{LT}) on hydrogen pressure at different time intervals. T_{high} = 475 K, T_m = 300 K and T_{low} = 283 K.

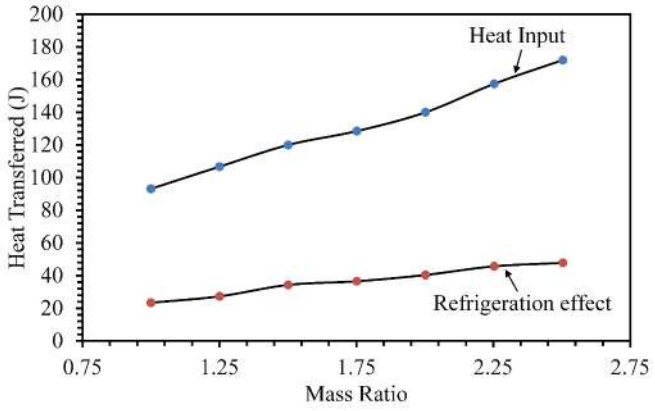

Fig. 11. Effect of mass ratio (M_{HT}/M_{LT}) on the heat input and refrigeration effect. T_{high} = 475 K, T_m = 300 K and T_{low} = 283 K.

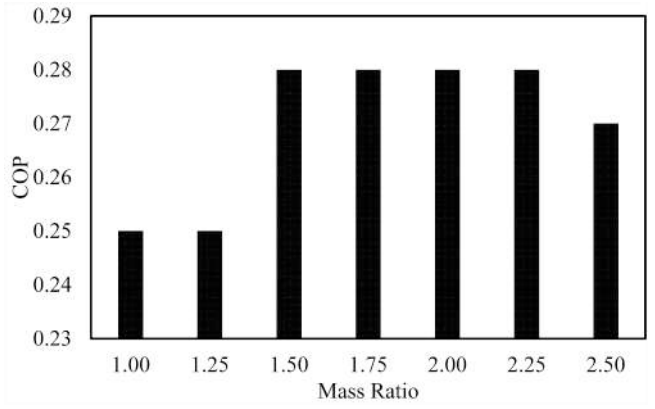

Fig. 12. Effect of mass ratio (M_{HT}/M_{LT}) on the COP. T_{high} = 475 K, T_m = 300 K and T_{low} = 283 K.

valve is closed and there is no transfer of hydrogen between the reactors. After this process, the equilibrium pressure in reactor B will be much higher than that in reactor A. At 160 s, the valve is opened and due to the pressure differential hydrogen gets desorbed from reactor B and gets absorbed in reactor A. The cooling effect is obtained during this process from LT side. Valve is closed and the reactors are heated to their initial temperatures. The gas pressure is continuously evolving so the pressure differential which is the driving potential changes with time. This leads to difference in sorption rates for different mass ratios at a given time.

Figs. 8a and 8b, represent the surface temperature of HT and LT sides for a mass ratio of 1.5 at different time durations. As shown in Fig. 8a, at a time duration of 10 s, the heat of reaction is supplied by the heat transfer fluid. The inlet air temperature is at 475 K while the minimum bed temperature is 466 K. At 130 s the system undergoes cooling. The inlet air temperature is kept at 300 K. At 170 s, hydrogen is desorbed from reactor B and absorbed in reactor A. The reactor is cooled using air at 300 K. After refrigeration, the reactor is heated to initial conditions. As shown in Fig. 8b, at a time duration of 10 s, hydrogen is absorbed in reactor B. Air at 300 K is used to cool the reactor to improve absorption. At 130 s, the reactor is sensibly cooled by air at 283 K. The minimum temperature of reactor reaches 305 K. At 170 s, the maximum refrigeration effect is achieved and a minimum bed temperature of 279 K is obtained. After refrigeration, the reactor is sensibly heated to initial conditions.

Fig. 9, represents the variation of bed temperatures for different mass ratios with time. For reactor A, the heat of reaction is supplied by the heat transfer fluid during regeneration. The heat input is at 475 K. As a result of this high heat input, the temperature of reactor A increases (T1). The temperature rise depends on the initial reaction rate. The temperature increases and tends to attain the air temperature. The temperature of reactor B increases while absorbing hydrogen and gradually approach the air temperature. The rise in temperature is due to the low thermal conductivity of hydride bed. The temperature of reactor B during refrigeration (T2) suddenly drops and gradually attains the heat transfer fluid temperature. This drop depends on the initial reaction rate. The bed temperature depends on the amount of hydrogen desorbed, heat of reaction and amount of heat transferred by the heat transfer fluid. As the mass ratio increases the heat of reaction increases, so the temperature drop also increases.

Fig. 10, shows the hydrogen pressure in the metal hydride based coupled beds across a cycle. For regeneration and refrigeration, the hydrogen pressure in both reactors is similar to the equilibrium pressure of desorbing alloy. Equilibrium pressure is a function of the bed temperature. P1 shows the hydrogen pressure during regeneration. As pressure differential increases, more hydrogen will be desorbed from reactor A. As more hydrogen is desorbed, it will have a negative effect on the driving potential but will enhance absorption in reactor B. Hydrogen pressure is continuously evolving so the driving potential also changes with time. P2, shows the hydrogen pressure during refrigeration. The maximum pressure differential is observed at the start of reaction and it gets reduced as hydrogen is desorbed from the reactor bed. The pressure differential increases as MR increases at the start of reaction. The increment in driving potential decreases after MR = 2.25. Further increase in MR, will only result in a small increment in the amount of hydrogen desorbed from reactor B.

3.2. *Effect of mass ratio on the performance of coupled bed*

Fig. 11, shows the variation of heat input and the refrigeration effect obtained for different mass ratios ratio (M_{HT}/M_{LT}). As the mass ratio is increased, the amount of hydrogen transferred between the reactors increases. The increase in the amount of cycled hydrogen increases the refrigeration effect and heat input. Fig. 12, represents the effect of mass ratio on the COP of the system. For a mass ratio MR = 1.5 to MR = 2.25, the increase in refrigeration effect dominates the increase in heat input. This region shows maximum COP. The difference between the mass of hydrogen desorbed in rector B and absorbed in reactor A is least for this range of mass ratios. After that, the mass of hydrogen transferred does not increase but the heat input increases which leads to a reduction in COP. The maximum COP obtained is 0.28.

4. Conclusions

Numerical simulation of a metal hydride based coupled bed with the alloy pair, $LaNi_{4.7}Al_{0.3}$ - $La_{0.8}Ce_{0.2}Ni_5$ is conducted using COMSOL Multiphysics® commercial code. The numerical model is valid for stable alloy beds which adopts different valid assumptions to simplify the model. The model is validated against reported results. Hoewever long-term reliability of the device need to be proved under several charge–discharge cycles.

The effect of differential masses of HT and LT alloys on the performance of the system is studied. The effect of mass ratio on the hydrogen pressure and hydride concentration in the coupled bed is significant during the initial part of sorption. This has direct effect on the amount of hydrogen exchanged between the reactors. Higher quantum of HT alloy can be used to absorb hydrogen desorbed from LT alloy in short cycle time. There is an optimum mass ratio for a given capacity and cycle time. It is found that 12 % increase in COP (0.28) is obtained for a cycle time of 260 s and mass ratio of 1.5. This corresponds to minimum alloy weight ensuring effective transfer of hydrogen across HT-LT reactors.

CRediT authorship contribution statement

Biju John Koshy: Writing – original draft, Software, Methodology.

G. Mohan: Conceptualization, Supervision, Writing – review & editing. **M. Prakash Maiya:** Validation, Resources, Project administration, Funding acquisition.

Declaration of competing interest

The authors declare that they have no known competing financial interests or personal relationships that could have appeared to influence the work reported in this paper.

Data availability

Data will be made available on request.

Acknowledgments

This study is supported by the Department of Science and Technology, Government of India under MECSP 2017 scheme. The help rendered by Dr. K. Balasubramanian, NFTDC Hyderabad is greatly acknowledged.

References

[1] M.K. Kazi, F.M. Eljack, M. El-Halwagi, M. Haouari, Green hydrogen for industrial sector decarbonization: Costs and impacts on hydrogen economy in Qatar, *Comput. Chem. Eng.* 145 (2021) 107144, https://doi.org/10.1016/j.compchemeng.2020.107144.

[2] C. Weckerle, M. Dörr, M. Linder, I. Burger, A compact thermally driven cooling system based on metal hydrides, Energies 13 (2020) 2482, https://doi.org/10.3390/en13102482.

[3] P. Muthukumar, M. Groll, Metal hydride based heating and cooling systems: A review, Int. J. Hydrogen Energy 35 (2010) 23817–23831, https://doi.org/10.1016/j.ijhydene.2010.01.115.

[4] E.I. Gkanas, C. Wang, S. Shepherd, O. Curnick, Metal-hydride-based hydrogen storage as potential heat source for the cold start of PEM FC in hydrogen-powered coaches: A comparative study of various materials and thermal management techniques, Hydrogen 3 (2022) 418–432, https://doi.org/10.3390/hydrogen3040026.

[5] A. Bandyopadhyay, K.D. Traxel, M. Lang, M.J.N. Eliaz, S. Bose, Alloy design via additive manufacturing: Advantages, challenges, applications and perspectives, Mater. Today 52 (2022) 207–224, https://doi.org/10.1016/j.mattod.2021.11.026.

[6] T. Nishizaki, K. Miyamoto, K. Yoshida, Coefficients of performance of hydride heat pumps, J. Less Common Mater. 89 (1983) 559–566, https://doi.org/10.1016/0022-5088.

[7] P. Dantzer, F. Meunier, What materials to use in hydride chemical heat pumps, Mater. Sci. Forum 31 (1988), https://doi.org/10.4028/www.scientific.net/MSF.31.1.

[8] T.G. Voskuilen, E.L. Waters, T.L. Pourpoint, A comprehensive approach for alloy selection in metal hydride thermal systems, Int. J. Hydrogen Energy 39 (2014) 13240–13254, https://doi.org/10.1016/j.ijhydene.2014.06.119.

[9] W. Supper, M. Groll, U. Mayer, Reaction kinetics in metal hydride reaction beds with improved heat and mass transfer, *J. Less –Common Met.* 104 (1984) 279–286, https://doi.org/10.1016/0022-5088(84)90412-0.

[10] N.A.A. Rusman, M. Dahari, A review on the current progress of metal hydrides material for soild-state hydrogen storage application, Int. J. Hydrogen Energy (2016) 1–19, https://doi.org/10.1016/j.ijhydene.2016.05.244.

[11] V.K. Sharma, E. Anil Kumar, Studies on La based intermetallic hydrides to determine their suitability in metal hydride based cooling systems, Intermetallics 57 (2015) 60–67, https://doi.org/10.1016/j.intermet.2014.10.004.

[12] V.K. Sharma, E. Anil Kumar, Measurement and analysis of reaction kinetics of La based hydride pairs suitable for metal hydride based cooling systems, Int. J. Hydrogen Energy (2014) 1–13, https://doi.org/10.1016/j.ijhydene.2014.09.083.

[13] J.H. Van't Hoff, Die Rolle des osmotischen druckes in der analogie zwischen lösungen und gasen, Z. Physik. Chem. 1 (1887) 481–508, https://doi.org/10.1515/zpch-1887-0151.

[14] V.K. Sharma, E. Anil Kumar, Effect of measurement parameters on thermodynamic properties of La-based metal hydrides, Int. J. Hydrogen Energy 39 (2014) 5888–5898, https://doi.org/10.1016/j.ijhydene.2014.01.174.

[15] A. Satheesh, P. Muthukumar, A. Dewan, Computational study of metal hydride cooling system, Int. J. Hydrogen Energy 34 (2009) 3164–3172, https://doi.org/10.1016/j.ijhydene.2009.01.083.

[16] B. Satya Sekhar, P. Muthukumar, Performance analysis of a metal hydride based heat transformer, Int. Energy J. 13 (2012) 29–44. http://203.159.5.126/index.php/reric/article/view/934.

[17] A. Satheesh, P. Muthukumar, Performance investigations of a single stage metal hydride heat pump, Int. J. Hydrogen Energy 35 (2010) 6950–6958, https://doi.org/10.1016/j.ijhydene.2010.04.043.

[18] A. Satheesh, P. Muthukumar, Simulation of double stage double effect metal hydride heat pump, Int. J. Hydrogen Energy 35 (2010) 1474–1484, https://doi.org/10.1016/j.ijhydene.2009.12.027.

[19] K. Malleswararao, N. Aswin, S. Srinivasa Murthy, P. Dutta, Studies on long-term and buffer modes of operations of a thermal energy storage system using coupled metal hydrides, Energy 258 (2022) 124868, https://doi.org/10.1016/j.energy.2022.124868.

[20] K. Malleswararao, N. Aswin, S. Srinivasa Murthy, P. Dutta, Performance prediction of a coupled metal hydride based thermal energy storage system, Int. J. Hydrogen Energy 45 (2020) 16239–16253, https://doi.org/10.1016/j.ijhydene.2020.03.251.

[21] A. d'Entremont, C. Corgnale, B. Hardy, R. Zidan, Simulation of high temperature thermal energy storage system based on coupled metal hydrides for solar driven steal power plants, Int. J. Hydrogen Energy 43 (2018) 817–830, https://doi.org/10.1016/j.ijhydene.2017.11.100.

[22] S. Srinivasa Murthy, Heat and mass transfer in solid state hydrogen storage: A review, J. Heat Transf. (134) 031020-1-11. 10.1115/1.4005156.

[23] S.A. Cetinkaya, T. Disli, G. Soyturk, O. Kizilkan, C. Ozgur Colpan, A review on thermal coupling of metal hydride storage tankswith fuel cells and electrolyzers, Energies 16 (2023) 341, https://doi.org/10.3390/en16010341.

[24] C. Weckerle, I. Burger, M. Linder, Novel reactor design for metal hydride cooling systems, Int. J. Hydrogen Energy (2017) 8063–8074, https://doi.org/10.1016/j.ijhydene.2017.01.066.

[25] C. Weckerle, I. Burger, M. Linder, Numerical optimization of a plate reactor for a metal hydride open cooling system, Int. J. Hydrogen Energy (2019) 16862–16876, https://doi.org/10.1016/j.ijhydene.2019.04.260.

[26] S. Kumar, P. Dutta, S. Srinivasa Murthy, Y.I. Aristov, L. Gordeeva, T.X. Li, R. Z. Wang, Studies on a metal hydride based year round comfort heating and cooling system for extreme climates, Energy Build. 244 (2021) 111042, https://doi.org/10.1016/j.enbuild.2021.111042.

[27] A. Zuttel, Hydrogen storage methods, Sci. Nat. 91 (2004) 157–172, https://doi.org/10.1007/s00114-004-0516-x.

[28] D.O. Dunikov, D.V. Blinov, A.M. Bozieva, A.N. Kazhakov, A.A. Krapivina, I. A. Romanov, E.V. Zadneprovskaya, S.I. Allakhverdiev, Permeability of a deformable metal hydride bed during hydrogen absorption, Int. J. Hydrogen Energy 51 (Part D) (2024) 375–387, https://doi.org/10.1016/j.ijhydene.2023.05.224.